maximum correlation coefficient for three different probe combinations. From this, the equivalent bedform migration rate is calculated, giving an average bedform migration of 4.6x10^{-4} ms^{-1}.

Table 2. Bedform migration rates calculated from lagged data.

Probes	Distance between probes (m)	Lag Time (s)	Correlation coefficient (r^2)	Migration rate (x 10^{-4} ms^{-1})
Probe 3 to Probe 1	0.06	133	0.8672	4.5
Probe 3 to Probe 2	0.03	61	0.9495	4.9
Probe 2 to Probe 1	0.03	67.5	0.8857	4.6

For a single measurement, the bed elevation is given to the nearest 2.5 mm which is the vertical extent of the measurement bins. To analyze the data, bed elevations were averaged over a period equivalent to a distance traveled of approximately 0.01m which is equivalent to averaging over 21.5 seconds. Figure 2 shows the bed profiles with the mean bedform migration rate being used to shift the time series to measure co-incident points of the bedform. The average bedform height measured using probe 1 is approximately 5 mm lower than for probes 2 and 3 (Table 3). Experiments carried out in still water with no sediment transport show that the different frequency probes show no more than a 0.5 mm difference in average bed elevation. This suggests that either the higher frequency transducers (probes 2 and 3) are not able to detect the true bed level due to higher sediment concentrations in a layer above the bed or that the lower frequency transducer (probe 1) penetrates the bed when sediment is being transported and measures below the true bed level.

Table 3. Bed elevation statistics for each probe. The average error range is the average of 95% confidence interval for the prediction of the mean bed height for each 1 cm unit of the bed.

Probes	Average bed elevation (mm)	Average Error range (mm)
Probe 1 (1 MHz)	60.46	±0.98
Probe 2 (2 MHz)	65.13	±0.47
Probe 3 (4 MHz)	65.64	±0.33

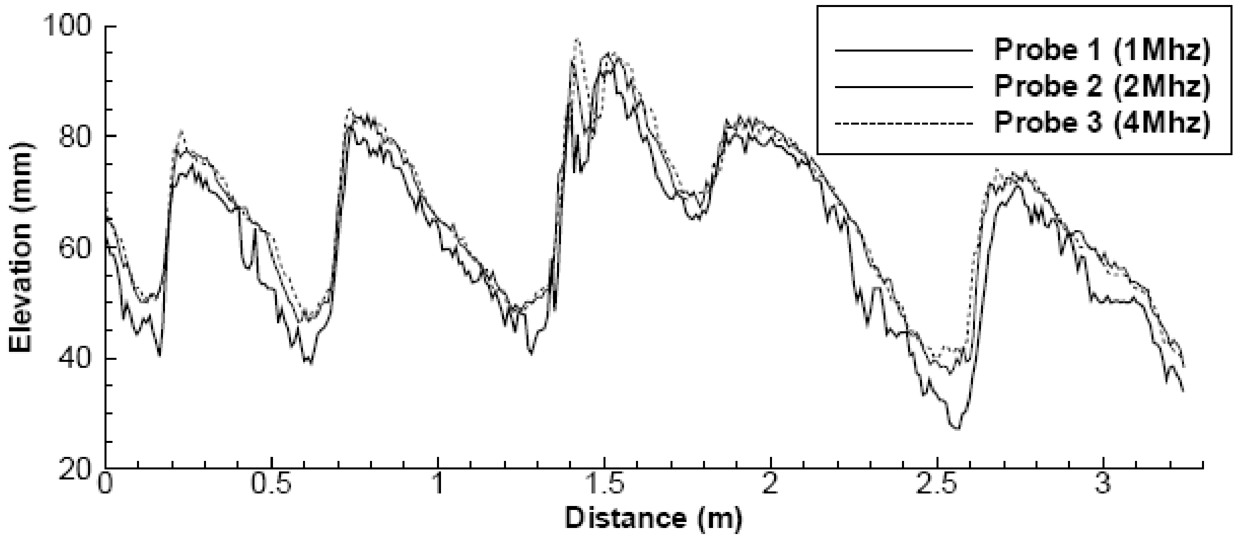

Figure 2. Bed profile measured by each probe. Data are averaged over a time period representing 1cm of movement and offset to account for the different probe positions

Spatial Distribution of Bedload Transport

If there is any variation in particle size, it is most likely to occur near the bed which may result in a different response from the higher and lower frequency transducers (the lowest frequency being more sensitive to larger sized sediment and *vice versa* for the higher frequency transducer). Hence, it can be assumed that the lower frequency probe will be most sensitive to the largest sediment which is likely to be transported as bedload and the first measurement bin above the bed should give the best representation of the variation of sediment concentration in the near-bed region, unless this probe returns measurements from below the bed surface. The acoustic data were averaged over the same period as the bed morphology data (21.5 seconds) which gives an estimated standard error of 1.3% from Equation 5. Figure 3 shows the distribution of sediment concentration detected by probe 1 in the layer immediately above the bed (the measurement bin immediately above the bin in which the maximum V is measured). There is considerable temporal fluctuation in the acoustic signal and the fluctuations above and below the mean value show limited correlation ($r^2 = 0.13$) to the bed topography. The most notable feature is that for most bedforms the sediment concentration peaks before the crest of that bedform and then shows a significant decrease towards the base of the lee slope of the bedform. Given the poor correlation between the bed morphology and the sediment concentration measurements it suggests that this measurements are potentially of limited use for understanding bedload transport and that they may be dominated by erroneous surface or sub-surface acoustic reflections.

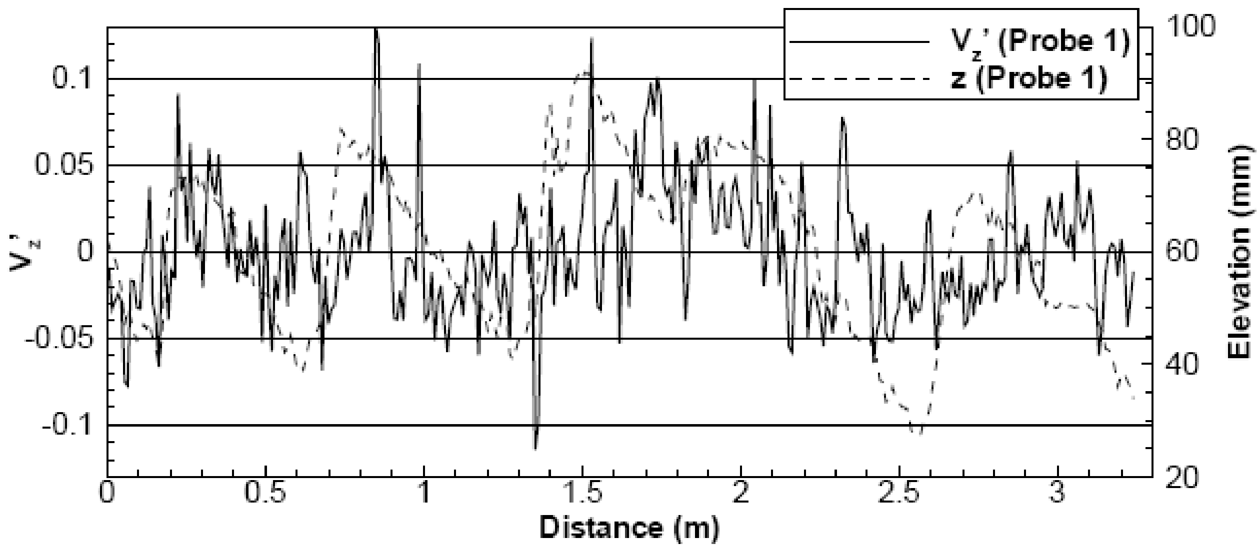

Figure 3. Sediment transport measured by probe 1 in the bin immediately above the detected bed surface. The bed profile measured by probe 1 is also shown.

Probe 3 uses the highest acoustic frequency and detects the bed with an elevation 5 mm greater than probe 1 (as described above). Figure 4 shows the variation in sediment concentration detected by probe 3 at the height where the maximum *V* is measured by probe 3. This is approximately 5 mm above the bed height detected by probe 1. There is a very noticeable correlation ($r^2 = 0.72$) between the bed elevation and the sediment concentration with concentrations that are greater than the mean occurring towards the crest of the bedform and concentrations that are lower than the mean in the troughs of the bedforms.

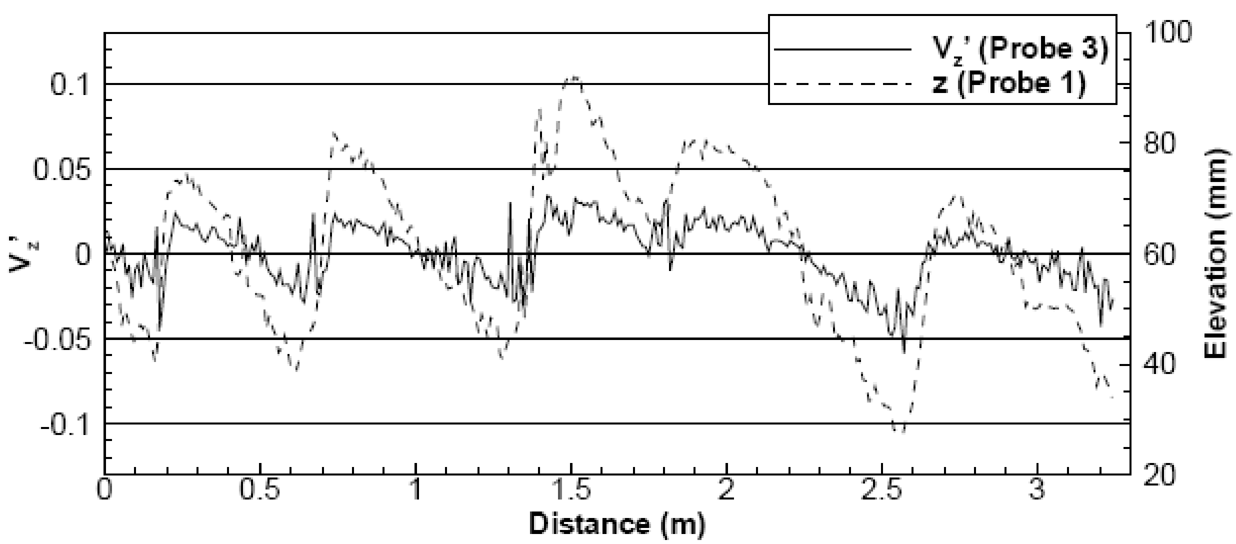

Figure 4. Sediment transport measured by probe 3 in the lowest measured bin. The bed profile measured by probe 1 is also shown.

The instantaneous bedload transport rate at a specific point ($q_b(x,t)$) can be estimated from the bedform morphology using the following equation:

$$q_b(x,t) = c(z(x,t) - z_0) \qquad \text{Equation 6}$$

where c is the migration rate of the bedform $z(x,t)$ is the bed elevation and z_0 is the height of the bedform where $q_b(x,t) = 0$ (e.g. Hoekstra et al., 2004; Engel and Lau, 1980). It can be assumed that z_0 is the average bed height. Figures 5A and B shows the relationship between $q_b(x,t)$ and the sediment concentration measured by probes 1 and 3. There is a poor fit between the instantaneous bedload transport calculated from the bedform morphology and the sediment concentration detected by probe 1 (Figure 5A) which suggests that this frequency is not well-suited to measurement of the transport rate near the bed. In contrast there is a strong relationship between the sediment concentration measured by probe 3 and the morphological estimate of the bedload transport rate (Figure 5B), indicating that either it is measuring the concentration of the bedload transport layer or that the near-bed suspended sediment concentration shows a strong correlation to the bedload transport rate.

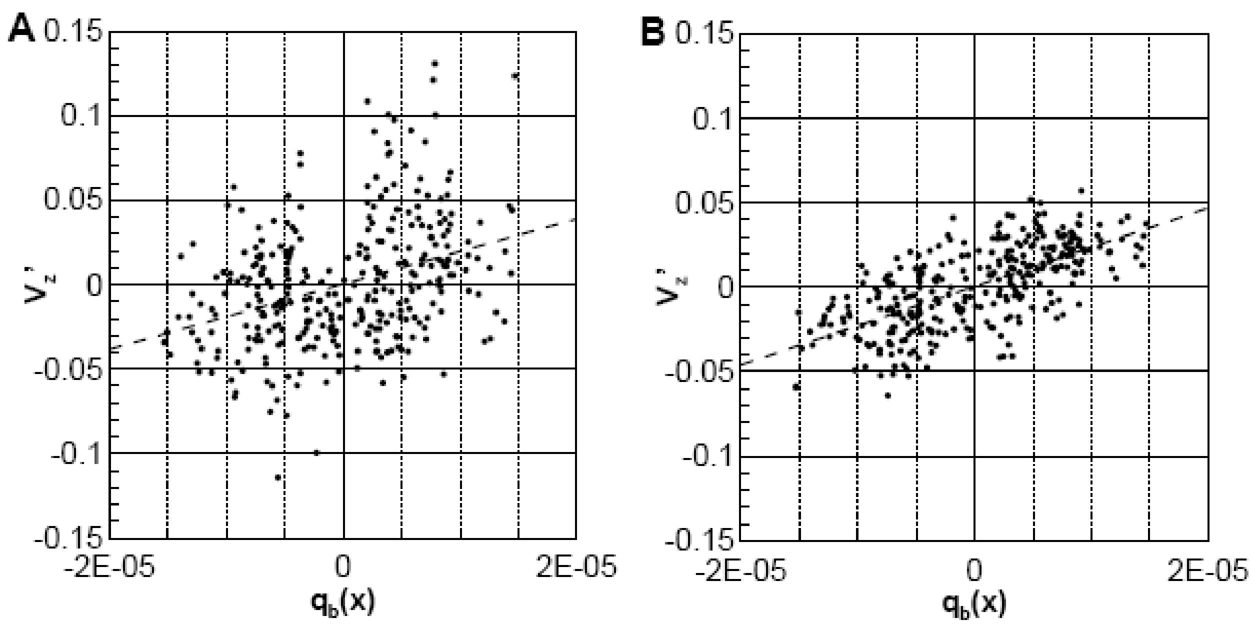

Figure 5A & B. Comparison of sediment transport rate calculated using morphological data ($q_b(x)$) with sediment transport measured by (a) probe 1 and (b) probe 3. The lines shown are calculated from linear regression and have an r^2 of 0.13 and 0.72 for probes 1 and 3 respectively. Data from probes 1 and 3 are taken from same location relative to bed as shown in Figures 3 and 4 respectively.

Spatial distribution of Suspended Sediment Concentration

Figures 6A, B and C show the temporal and spatial distribution of backscatter deviation for each of the three probes. It would appear that probe 1 is most sensitive to changes near the bed and clearly shows pulses of higher sediment concentration near the bed. There is a noticeable increase in concentration immediately on the lee slope of each bedform. Probes 2 and 3 appear to show higher sediment concentration above the crests and lower sediment transport in the trough regions. Sediment concentration detected by probe 3 in the lee of the bedforms is noticeably different from that shown by probe 1. The data from probe 3 show that an area of higher sediment concentration separates from the bed and is carried some distance downstream from the bedform crest, whilst the increase in sediment concentration detected by probe 1 remains close to the bed surface. There are smaller fluctuations in suspended sediment concentrations over the last bedform measured compared to the earlier bedforms. Figure 7 shows the first three bedforms in more detail with the measurements taken by probe 3. This clearly shows a significant increase in concentration in the lee of the bedform crest which appears to show pulses of higher sediment transport downstream from the dune crest and a significant reduction in concentration towards the base of the trough.

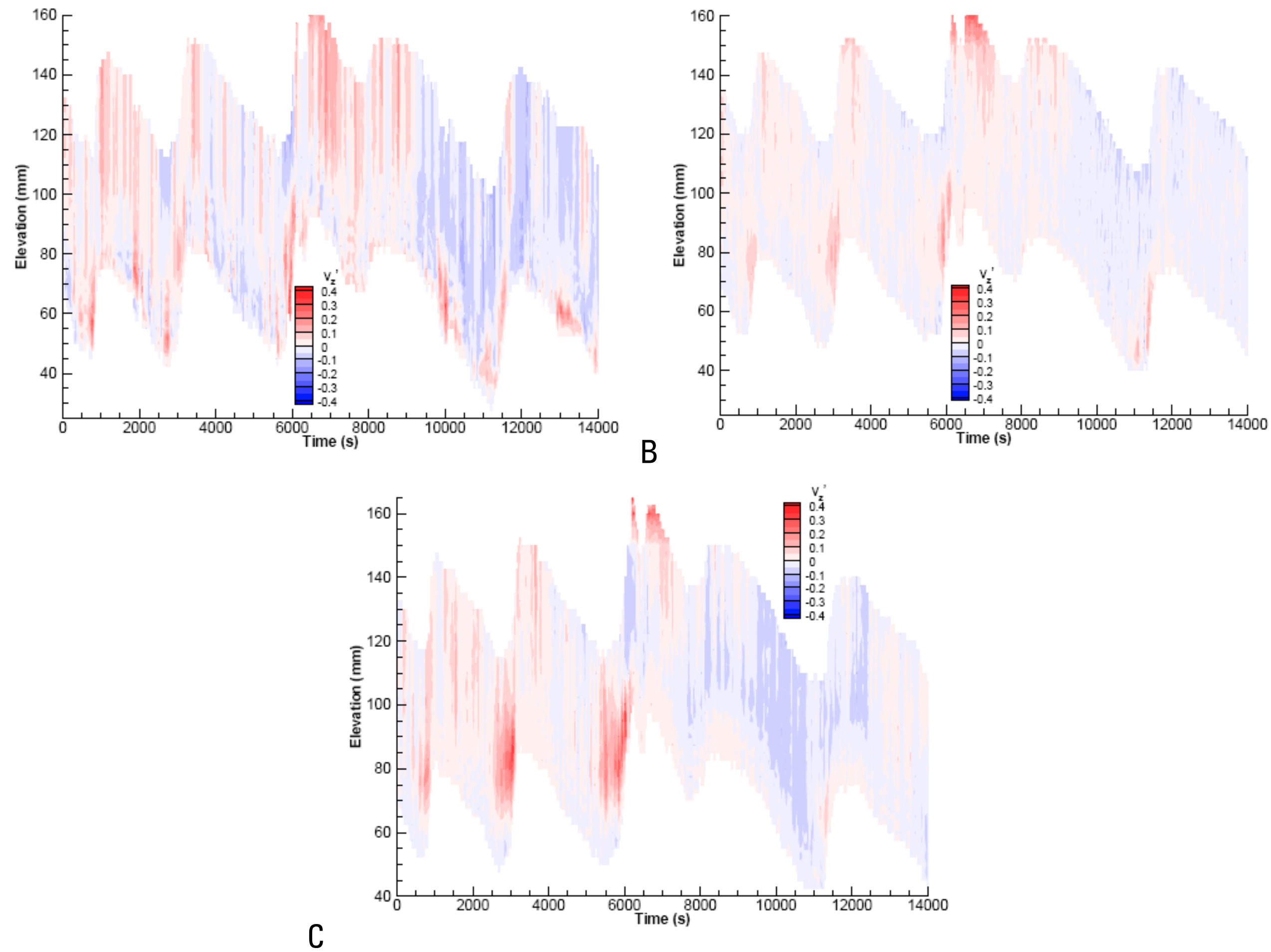

Figure 6 A, B & C. Contour plots showing sediment transport measured by probe 1 (A), probe 2 (B) and probe 3 (C). Data are shown only for the bins where there is a complete record through the entire time series. Bedform is shown by grey shaded area. Note that the fluctuations are normalized such that variations in sediment transport with height are removed.

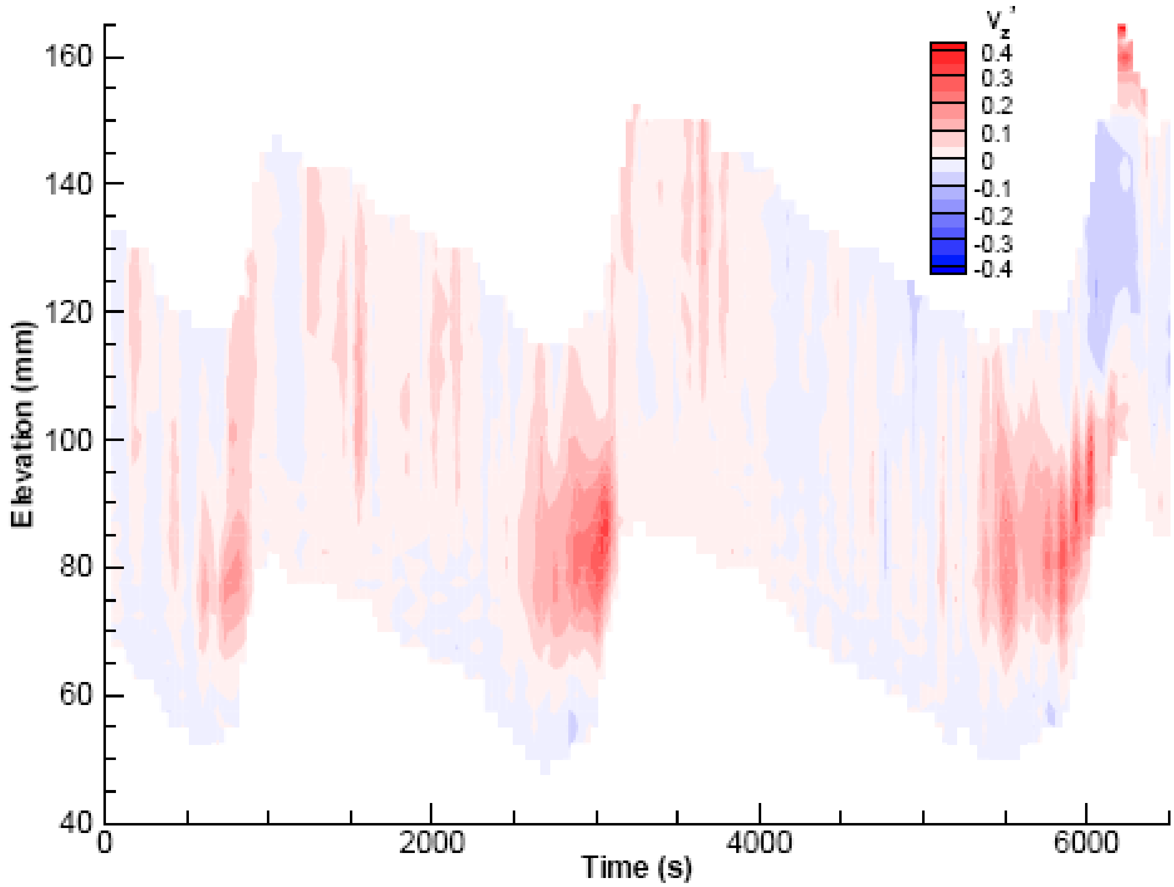

Figure 7. Detail showing the first three bedforms shown in Figure 6C.

Discussion and Summary of Technique

Acoustic backscatter profiling appears to have considerable potential for identifying spatial and temporal fluctuations in sediment concentration over bedforms. The morphological data that are obtained show the detailed structure of the passage of bedforms which can be used to obtain the bedform migration rate from multiple probes. This allows the bedload transport rate to be calculated based on the rate of sediment transport per unit width of the flume. Indeed, this shows very good correlation with the higher frequency measurement of the sediment transport in the near-bed layer which may have some potential for calibrating the results. There is not a clear relationship between the sediment transport detected just above the bed by the lowest frequency probe suggesting that either this signal is affected by noise from surface or below-bed acoustic reflections or that sediment transport in this region is discontinuous and is affected by short-time scale variations in flow properties such as turbulent events. Significant peaks in sediment transport occur ‘upstream’ from each crest and there is a marked decrease towards the trough. Downstream from the base of the lee slope there are periodic increases in transport which may reflect fluctuations in the reattachment point (e.g. Bennett and Best, 1996, Ha and Chough, 2003).

The spatial distribution of the acoustic response shows the structure of sediment concentration over several bedforms (Figure 6). The spatial distribution of the fluctuations in the acoustic signal show greater sediment concentration over the stoss slopes where flow is accelerated and reduced sediment concentrations in the trough regions which is similar to the pattern of sediment concentration measured by Kostaschuk and Villard (1999) using a pump sampling system. Regions of higher sediment concentrations in the lee of the bedform are detected by the high frequency probe; these regions are detached from the bed as shown by the relatively low sediment concentrations towards the base of the bedform trough (Figure 7). This suggests that sediment may be transported from the crest of the bedform into the main body of the flow. This may reflect the detachment of particles from the bed at the bedform crest, in a process similar to that shown by Ha and Cough (2003) based on motion picture analysis. Kostaschuk and Villard (1999) also demonstrated the presence of strongly intermittent suspension events using an acoustic profiler, which is similar to the fluctuations in higher sediment concentration downstream from the crest of the bedform. The latter also show some periodicity that may reflect turbulent fluctuations in the shear layer development. These suspension structures and intermittent increases in sediment entrainment have been associated with turbulent ejections forming at the bedform crest (e.g. Kostachuk and Villard, 1999). The near-bed sediment transport shown by the high frequency probe also shows a significant increase in transport on the stoss slope (Figure 4) which may reflect the entrainment of sediment at the point of reattachment of the separation zone (e.g. Bennett and Best, 1996, Kostaschuk and Villard, 1999, Ha and Chough, 2003).

The use of multiple probes allows rapid calculation of morphologically-based transport rate. However, further work needs to be carried out to calibrate the system to quantify the spatial and temporal characteristics of suspended sediment transport. This is likely to be possible in terms of calculating sediment concentration which can be quantified using a single frequency; however the spatial separation of the probes means that it is unlikely to be suitable for determining sediment size variations at this scale. Due to the small distance of the bed surface from the probe, the acoustic signal returned from the bed is very strong. Therefore to avoid saturation of the signal, very low gains need to be used when collecting the data which may lead to problems detecting the true bed level.

Acknowledgements

I am very grateful to David Gaeuman and James Chambers for their constructive comments which have greatly improved this paper.

References Cited

Bennett, S.J. and Best, J.L. 1996. Mean flow and turbulence structure over fixed ripples and the ripple-dune transition, in Ashworth, P.J., Bennett, S.J., Best, J.L. and McLelland, S.J. (Eds.) Coherent Flow Structures in Open channels, Wiley, Chichester, UK, pp. 281-304.

Crawford, A.M. and Hay, A.E., 1993. Determining suspended sand size and concentration from multifrequency acoustic backscatter, Journal of the Acoustical Society of America, 94 (6), pp. 3312–3324.

Engel, P. and Lau, Y.L., 1980, Computation of bedload using bathymetric data. Journal of the Hydraulics Division, 106, pp. 369–380.

Hoekstra, P., Bell, P., van Santen, P., Rood, N., Levoy, F. and Whitehouse, R, 2004, Bedform migration and bedload transport on an intertidal shoal, Continental Shelf Research, 24, 11, pp. 1249-1269.

Ha H.K. and Chough S.K., 2003, Intermittent turbulent events over sandy current ripples: a motion-picture analysis of flume experiments, Sedimentary Geology, 161 (3-4), pp. 295-308.

Kostaschuk, R. and Villard P., 1999, Turbulent sand suspension over dunes, in Smith N.D. and Rogers J. (Eds.), Fluvial Sedimentology VI, Special publication of the International Association of Sedimentologists, 28, pp. 3-13.

Libicki, C., Bedford, K.W., and Lynch, J.F., 1989, The interpretation and evaluation of a 3-Mhz acoustic backscatter device for measuring benthic boundary layer sediment dynamics. Journal of the Acoustical Society of America, 85 (4), pp. 1501-1511.

Smerdon, A.M., Rees, J.M. and Vincent, C.E., 2004, An acoustic backscatter instrument to measure near-bed sediment processes, Accessed 12th March 2007 at: http://www.aquatecgroup.com/download/datasheet/aquascat/ABSPaper.pdf

Thorne, P.D. and Hanes, D.M., 2002, A review of acoustic measurement of small-scale sediment processes, Continental Shelf Research, 22, pp. 603–632.

Thorne, P.D. and Hardcastle, P.J., 1997, Acoustic measurements of suspended sediments in turbulent currents and comparison with in-situ samples. Journal of the Acoustical Society of America, 101 (5)(Pt. 1), pp. 2603–2614.